

X -States From a Finite Geometric Perspective

Colm Kelleher¹, Frédéric Holweck², Péter Lévay³, and Metod Saniga⁴

¹*Institut de Mathématiques de Bourgogne, UMR 5584, Université de Bourgogne Franche-Comté, F-21078 Dijon, France*

²*Laboratoire Interdisciplinaire Carnot de Bourgogne, ICB/UTBM, UMR 6303 CNRS, Université Bourgogne Franche-Comté, F-90010 Belfort, France*

³*MTA-BME Quantum Dynamics and Correlations Research Group, Department of Theoretical Physics, Budapest University of Technology and Economics, 1521 Budapest, Hungary*

⁴*Astronomical Institute of the Slovak Academy of Sciences, SK-05960 Tatranská Lomnica, Slovakia*

March 2, 2022

Abstract

It is found that 15 different types of two-qubit X -states split naturally into two sets (of cardinality 9 and 6) once their entanglement properties are taken into account. We characterize both the validity and entangled nature of the X -states with maximally-mixed subsystems in terms of certain parameters and show that their properties are related to a special class of geometric hyperplanes of the symplectic polar space of order two and rank two. Finally, we introduce the concept of hyperplane-states and briefly address their non-local properties.

1 Introduction

Two-qubit X -states are usually introduced in the literature as two-qubit density matrices with an X -shape,

$$\rho = \begin{pmatrix} \rho_{11} & 0 & 0 & \rho_{14} \\ 0 & \rho_{22} & \rho_{23} & 0 \\ 0 & \rho_{32} & \rho_{33} & 0 \\ \rho_{41} & 0 & 0 & \rho_{44} \end{pmatrix}. \quad (1)$$

The EPR-states and the Werner states are particular cases of X -states [8] and their properties have extensively been studied from quantum information theoretic perspective [18, 1]. It was A.R.P. Rau who first pointed out, in a series of papers [11, 17, 12], the underlying algebraic structure defining an X -state. Taking X, Y, Z to represent the usual Pauli matrices and I to be the identity matrix, Eq. (1) can be rewritten in the following way

$$\rho = \frac{1}{4}(I \otimes I + \tau^A Z \otimes I + \tau^B I \otimes Z + \beta_{zz} Z \otimes Z + \beta_{xx} X \otimes X + \beta_{yy} Y \otimes Y + \beta_{yx} Y \otimes X + \beta_{xy} X \otimes Y), \quad (2)$$

where τ 's and β 's are real coefficients that can be calculated from ρ_{ij} . Rau also noticed that the non-trivial two-qubit operators involved in Eq. (2) have the algebraic structure of the projective plane of order two, the Fano plane, if one considers their products (Figure 1).

Up to a phase factor, there are 15 non-trivial two-qubit observables and, therefore, 15 labeled Fano planes similar to that depicted in Figure 1, each of them hosting a maximal set of observables commuting with a given one. Rau [11] further suggested to extend the definition of X -states to all two-qubit density matrices that would yield similar underlying Fano structures once decomposed on a particular two-qubit Pauli basis.

In this article we consider the 15 different kinds of X -states following Rau's idea and show that they split into two groups. Group 1 consists of X -like states that are always separable irrespectively of the choice of parameters τ 's and β 's. Group 2 entails X -states that can be entangled if the parameters satisfy certain

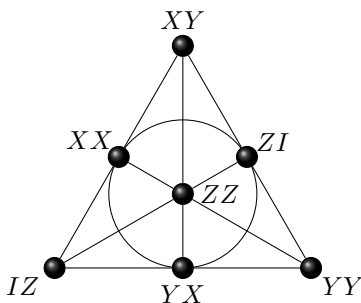


Figure 1: Up to a phase, the multiplication properties of the 7 operators of Eq. (2). They form a Fano plane. The three lines intersecting at ZZ correspond to three sets of mutually commuting operators. One notices that the distinguished observable $Z \otimes Z$ commutes with all the remaining ones. (AB is a short-hand for $A \otimes B$). All 15 Fano planes of $\text{PG}(3,2)$ are explicitly listed in Appendix A.

conditions. The standard X -state given by Eq. (1) and Eq. (2) belongs to Group 2. For Group 2 X -states with maximally mixed subsystems, we also give explicit constraints on their parameters to decide on the validity and entanglement of particular states. Then one proposes an alternative finite-geometric definition of X -states making use of a particular type of geometric hyperplanes – so-called perp-sets – of the symplectic polar space of order two and rank two, $\mathcal{W}(3,2)$. The existence of two distinct groups of X -states is here embodied in the intersection properties of perp-sets with a specific hyperbolic quadric of $\mathcal{W}(3,2)$. This then naturally leads to a generalization of X -states for all the remaining types of hyperplanes of $\mathcal{W}(3,2)$, with subsequent analysis of their entanglement properties. Finally, we briefly address non-local properties for X -states of Group 2 as well as for the other hyperplane-states that can produce entangled states.

Symbols and Notation. Let $\mathcal{P}_2 = \{sA_1 \otimes A_2, A_i \in \{I, X, Y, Z\}, s \in \{\pm 1, \pm i\}\}$ be the group of two-qubit Pauli observables where $X = \begin{pmatrix} 0 & 1 \\ 1 & 0 \end{pmatrix}$, $Y = \begin{pmatrix} 0 & -i \\ i & 0 \end{pmatrix}$ and $Z = \begin{pmatrix} 1 & 0 \\ 0 & -1 \end{pmatrix}$, I being the identity matrix. As already mentioned, the tensor product of observables will be shorthanded as $A_1 \otimes A_2 = A_1 A_2$. Disregarding a phase factor, $\pm 1, \pm i$, the 15 nontrivial two-qubit Pauli operators can be identified with the 15 points of the projective space over the two element field, $\text{PG}(3,2)$, as follows. Let $A_1 = Z^{\mu_1} \times X^{\nu_1}$ and $A_2 = Z^{\mu_2} \times X^{\nu_2}$ be two Pauli matrices and $A_1 A_2 = (Z^{\mu_1} \times X^{\nu_1})(Z^{\mu_2} \times X^{\nu_2})$. Then $A_1 A_2$ is a non-trivial two qubit Pauli operator iff $(\mu_1, \nu_1, \mu_2, \nu_2)$ is a nonzero vector of V^4 , the four-dimensional vector space over the two element field $\text{GF}(2) = \{0, 1\}$, and thus can be mapped to a point of $\text{PG}(3,2)$:

$$\pi : \begin{cases} \mathcal{P}_2 \setminus I_2 & \rightarrow \text{PG}(3,2), \\ s(Z^{\mu_1} \times X^{\nu_1})(Z^{\mu_2} \times X^{\nu_2}) & \mapsto [\mu_1 : \nu_1 : \mu_2 : \nu_2]. \end{cases} \quad (3)$$

For instance, the observables $\{IX, -IX, iIX, -iIX\}$ are mapped to the point $[0 : 0 : 0 : 1]$ and $\{YZ, -YZ, iYZ, -iYZ\}$ are mapped to the point $[1 : 1 : 1 : 0]$. A line of $\text{PG}(3,2)$ is made of triplets of points (p, q, r) such that $r = p + q$. The corresponding classes of two-qubit operators $\overline{\mathcal{O}}_p, \overline{\mathcal{O}}_q, \overline{\mathcal{O}}_r$ satisfy $\overline{\mathcal{O}}_p \times \overline{\mathcal{O}}_q = \overline{\mathcal{O}}_r$. $\text{PG}(3,2)$ contains 15 Fano planes that can neatly be parametrized by the 15 points of $\text{PG}(3,2)$. Given a non-degenerate bilinear form

$$\sigma(p, q) = p_1 q_2 + p_2 q_1 + p_3 q_4 + p_4 q_3 \quad (4)$$

for $p = [p_1 : p_2 : p_3 : p_4]$ and $q = [q_1 : q_2 : q_3 : q_4] \in \text{PG}(3,2)$, one can define the 15 Fano planes of $\text{PG}(3,2)$ as $F_p = \{q \in \text{PG}(3,2), \sigma(p, q) = 0\}$. For instance, $F_{[1:0:1:0]} = \{[1 : 0 : 1 : 0], [0 : 1 : 1 : 1], [1 : 1 : 0 : 1], [0 : 0 : 1 : 0], [1 : 0 : 0 : 0], [0 : 1 : 0 : 1], [1 : 1 : 1 : 1]\}$; it is easy to see that this Fano plane is the one shown in Figure 1. For the convenience of the reader, the 15 different Fano planes of $\text{PG}(3,2)$ are given in terms of operators in Appendix A.

2 Entangled X -states split into two groups

Given a two-qubit system with density matrix ρ , its ‘entanglement status’ can be discerned from the fact whether the partial transpose ρ^Γ is positive-semidefinite, or not [3], where the partial transpose can be taken over any subsystem (PPT criterion). Namely, if ρ^Γ is positive-semidefinite the system is separable, otherwise it is entangled. In what follows a density matrix ρ is said to be *valid* iff it is positive-semidefinite.

If the 15 types of X -states are expressed in terms of Pauli operators (Eq. (2)), we find that 6 of them are endowed with 4 τ coefficients and 3 β ones; these are states that belong to Group 1. The 9 types of Group 2 entail states with 2 τ ’s and 5 β ’s. As already pointed out, the state given by Eq. (2) is from Group 2.

The eigenvalues λ_i of density matrices of Group 1 states are found to be equal to those of their partial transposes λ_i^Γ ,

$$\lambda_i = \lambda_i^\Gamma = \begin{cases} \frac{1}{4} \left(\tau_0 + 1 \pm \sqrt{(\beta_1 + \tau_1)^2 + (\beta_2 + \tau_2)^2 + (\beta_3 + \tau_3)^2} \right) \\ \frac{1}{4} \left(-\tau_0 + 1 \pm \sqrt{(\beta_1 - \tau_1)^2 + (\beta_2 - \tau_2)^2 + (\beta_3 - \tau_3)^2} \right), \end{cases} \quad (5)$$

where we have introduced generalised parameters for the 6 different states - the three β_i parameters correspond to three correlation operators sharing a common tensor factor, the three τ_i , $i = \{1, 2, 3\}$, correspond to the coordinates of the Bloch vector of one partially reduced state, and τ_0 is the coordinate of the Bloch vector of the remaining partially reduced state. For example, $F_{[0:0:0:1]}$ maps to the following Group 1 state:

$$\rho_{[0:0:0:1]} = \frac{1}{4} [I \otimes I + \tau_x^A X \otimes I + \tau_y^A Y \otimes I + \tau_z^A Z \otimes I + \tau_z^B I \otimes Z + \beta_{xz} X \otimes Z + \beta_{yz} Y \otimes Z + \beta_{zz} Z \otimes Z]. \quad (6)$$

As $\{\lambda_i\} = \{\lambda_i^\Gamma\}$, the positive-semidefinite criteria for ρ and ρ^Γ render all Group 1 states separable.

We can also introduce generalised parameters for Group 2 states:

$$\begin{aligned} (\tau_1, \tau_2) &= (\tau^A, \tau^B), \\ \beta_0 &:= \{\beta_{ij} | \beta_{ik} = 0 = \beta_{lj} \quad \forall k \neq i, l \neq j\}, \\ M &= \begin{pmatrix} \beta_1 & \beta_2 \\ \beta_3 & \beta_4 \end{pmatrix} := \beta(i, j) \quad \text{for } \beta_0 \neq \beta_{ij}, \end{aligned} \quad (7)$$

where τ_i are the coordinates of the Bloch vectors of the partially reduced states (always one nonzero coordinate for each subsystem), β_0 is the unique β parameter whose operator has no common factors with the other nontrivial operators, and M is the submatrix formed from the β matrix by removing the row and column containing β_0 . For the Eq. (2) example,

$$\begin{aligned} \beta &= \begin{pmatrix} \beta_{xx} & \beta_{xy} & & \\ \beta_{yx} & \beta_{yy} & & \\ & & & \beta_{zz} \end{pmatrix}, \\ M &= \begin{pmatrix} \beta_{xx} & \beta_{xy} \\ \beta_{yx} & \beta_{yy} \end{pmatrix}, \\ \beta_0 &= \beta_{zz}. \end{aligned}$$

In this construction, eigenvalues of the density matrix of a Group 2 state have two general forms:

TYPE I:

$$\begin{aligned} \lambda_{i,I} &= \begin{cases} \frac{1}{4} \left(\beta_0 + 1 \pm \sqrt{(\beta_1 - \beta_4)^2 + (\beta_2 + \beta_3)^2 + (\tau_1 + \tau_2)^2} \right), \\ \frac{1}{4} \left(-\beta_0 + 1 \pm \sqrt{(\beta_1 + \beta_4)^2 + (\beta_2 - \beta_3)^2 + (\tau_1 - \tau_2)^2} \right), \end{cases} \\ \lambda_{i,I}^\Gamma &= \begin{cases} \frac{1}{4} \left(\beta_0 + 1 \pm \sqrt{(\beta_1 + \beta_4)^2 + (\beta_2 - \beta_3)^2 + (\tau_1 + \tau_2)^2} \right), \\ \frac{1}{4} \left(-\beta_0 + 1 \pm \sqrt{(\beta_1 - \beta_4)^2 + (\beta_2 + \beta_3)^2 + (\tau_1 - \tau_2)^2} \right). \end{cases} \end{aligned} \quad (8)$$

Type II is obtained by the switch ($\lambda_i \leftrightarrow \lambda_i^\Gamma$), or, equivalently, by the transformations ($\beta_0 \mapsto -\beta_0$), ($\tau_{1(2)} \mapsto -\tau_{1(2)}$).

These forms allow for entangled states, and we will later show the corresponding conditions for states with maximally mixed subsystems. We also assign to each Group 2 X -state a parameter t to denote its type; $t = 1$ for Type I states, and $t = 2$ for Type II ones.

The parameters in λ, λ^Γ above can be expressed as coordinates in \mathbf{R}^2 , with the radical term giving the Euclidean distance between pairs of points. This handy representation will allow us to find regions of validity, separability and entanglement, using the following proposition:

Proposition 2.1. *Let $L^+ := \sqrt{(\beta_1 + \beta_4)^2 + (\beta_2 - \beta_3)^2}$ and $L^- := \sqrt{(\beta_1 - \beta_4)^2 + (\beta_2 + \beta_3)^2}$. For a valid, entangled generalised X -state ρ with $\tau_1 = \tau_2 = 0$ and eigenvalues $\lambda_{i,I} = \{1 \pm \beta_0(\pm)L^\mp\}$, $\beta_0 < 0 \iff L^+ > L^-$.*

Proof. (\implies): The validity constraint yields

$$1 - \beta_0 \geq L^+ \quad \text{and} \quad 1 + \beta_0 \geq L^-. \quad (9)$$

For $\beta_0 < 0$ and $\min\{\lambda_{i,I}^\Gamma\} < 0$,

$$1 - |\beta_0| < L^+ \leq 1 + |\beta_0| \quad \text{or} \quad 1 + |\beta_0| < L^- \leq 1 - |\beta_0|.$$

Only the left-hand-side inequalities are consistent, and can be combined with the validity conditions to give $L^- \leq 1 - |\beta_0| < L^+$.

(\Leftarrow): We have

$$\begin{aligned} 1 - \beta_0 &\geq L^+ > L^-, \\ \implies 1 + \beta_0 < L^+ \leq 1 - \beta_0 \quad \text{or} \quad 1 - \beta_0 < L^- \leq 1 - \beta_0, \end{aligned}$$

which again invalidates the right-hand-side inequalities, giving

$$-\beta_0 > \beta_0 \implies \beta_0 < 0.$$

□

Now, we can simply take $\beta_0 < 0$ and the PPT criterion acquires the form

$$1 - |\beta_0| < L^+. \quad (10)$$

Taking $\beta_0 > 0$ yields

$$1 - |\beta_0| < L^-. \quad (11)$$

This thus allows us to consider the $\beta_0 < 0$ case to determine the regions of validity, separability and entanglement, and then make suitable transformations for the $\beta_0 > 0$ case.

Proposition 2.2. *Let $C := (\beta_4, \beta_3), D := (\beta_1, \beta_2), E := (\beta_1, -\beta_2), F := (\beta_4, -\beta_3) \in \mathbf{R}^2$, $r := 1 - |\beta_0|$, $R := 1 + |\beta_0|$, and (C, r) be the closed disc centered at C with radius r , etc.*

For a given Group 2 X -state with maximally-mixed subsystems represented by ρ with given $\beta_0, \beta_3, \beta_4$, its region of validity is given by $\mathcal{V} := (C, r) \cap (-C, R)$, the region of separability by $\mathcal{S} := (C, r) \cap (-C, r)$, and the region of entanglement by $\mathcal{E} := \mathcal{V} \setminus \mathcal{S}$. The matrix ρ is valid iff $E \in (-1)^t \text{sgn}(\beta_0)\mathcal{V}$, separable for $E \in \mathcal{S}$, and entangled for $E \in (-1)^t \text{sgn}(\beta_0)\mathcal{E}$. The following conditions hold:

1. $\mathcal{V} \neq \emptyset \iff \beta_3^2 + \beta_4^2 \leq 1$;
2. $\mathcal{S} \neq \emptyset \iff \beta_3^2 + \beta_4^2 \leq (1 - |\beta_0|)^2$.

Equivalently, for a given generalised Group 2 X -state ρ with given $\beta_0, \beta_1, \beta_2$, its region of validity for F is given by $\mathcal{V}' := (E, r) \cap (-E, R)$, the region of separability by $\mathcal{S}' := (E, r) \cap (-E, r)$, and the region of entanglement by $\mathcal{E}' := \mathcal{V}' \setminus \mathcal{S}'$ with corresponding conditions:

1. $\mathcal{V}' \neq \emptyset \iff \beta_1^2 + \beta_2^2 \leq 1$;
2. $\mathcal{S}' \neq \emptyset \iff \beta_1^2 + \beta_2^2 \leq (1 - |\beta_0|)^2$.

ρ is valid iff $F \in (-1)^t \text{sgn}(\beta_0)\mathcal{V}'$, separable for $F \in \mathcal{S}'$, and entangled for $F \in (-1)^t \text{sgn}(\beta_0)\mathcal{E}'$.

Proof. We consider a state of Type I with maximally mixed subsystems, with $\beta_0 < 0$, and prove the first half of the proposition. The second half follows readily from the same chain of arguments. For validity, by Proposition 2.1, we have

$$L^+ \leq 1 + |\beta_0|, \quad (12a)$$

$$L^- \leq 1 - |\beta_0|. \quad (12b)$$

The quantity L^- (L^+) is given by the Euclidean distance between points C and E (C and $-E$). Via the representation of the parameters in \mathbf{R}^2 (see Figure 3), the condition (12b) means that the point E is contained within the closed disc (C, r) and, equally, that the point $-E$ lies in $(-C, r)$. Condition (12a) means that the point $-E$ is contained within (C, R) . Thus, for both to hold, $-E$ must lie within $(-C, r) \cap (C, R)$. Reflecting through the origin, this implies that $E \in \mathcal{V} := (C, r) \cap (-C, R)$. This region is nonempty when the points $C, -C$ are closer to each other than $r + R$, i.e. when $|C|^2 = \beta_4^2 + \beta_3^2 \leq 1$. For separability, we need that $\min\{\lambda_{i,I}^\Gamma\} \geq 0$, i.e. that $L^+ \leq 1 - |\beta_0|$. This gives $-E \in (C, r)$, or, equivalently, that $E \in (-C, r)$. For validity and separability that requires $E \in \mathcal{S} := (C, r) \cap (-C, r)$, which when reflected through the origin also gives $-E \in \mathcal{S}$. This region is nonempty when $|C|^2 \leq r^2 = (1 - |\beta_0|)^2$. For entanglement that occurs when the state is valid but not separable we obtain $E \in \mathcal{V} \setminus \mathcal{S}$. We note now that for the case $\beta_0 > 0$, via proposition 2.1, the conditions (12) exchange $L^+ \leftrightarrow L^-$, or, equivalently, $E \mapsto -E$. This does not affect the separability condition as \mathcal{S} is symmetric under these transformations, but it does change the sign of the regions \mathcal{V}, \mathcal{E} that E must belong to. Thus, by multiplying by the sign of β_0 we can cover both the scenarios. Finally, we note that under the transformation $\beta_0 \mapsto -\beta_0$ we can infer the conditions for Type II. As this sign change is equivalent to exchanging $L^+ \leftrightarrow L^-$ in proposition (2.1), it means that we must once again multiply by a factor of (-1) to exchange types. Then we see that $E \in (-1)^t \text{sgn}(\beta_0)\mathcal{V}$ covers our initial case and any of the mentioned transformations. \square

Remark 2.3. Proposition 2.2 provides a constructive way of generating examples of generalised X -states with maximally-mixed subsystems that are entangled as shown in Figures 2 and 3.

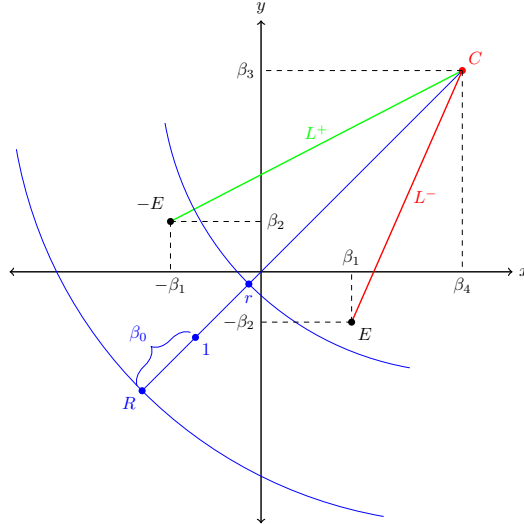


Figure 2: The parameter space for a positive-definite Group 2 state (i.e., a state with maximally-mixed subsystems and of Type I, $\beta_0 < 0$). The parameters β_1, β_4 are plotted on the x -axis, β_2, β_3 on the y -axis. As $E \in (C, r) \wedge -E \in (C, R)$, this state is valid as per proposition 2.2. Moreover, as $L^+ > r = 1 - |\beta_0|$, the state is also entangled.

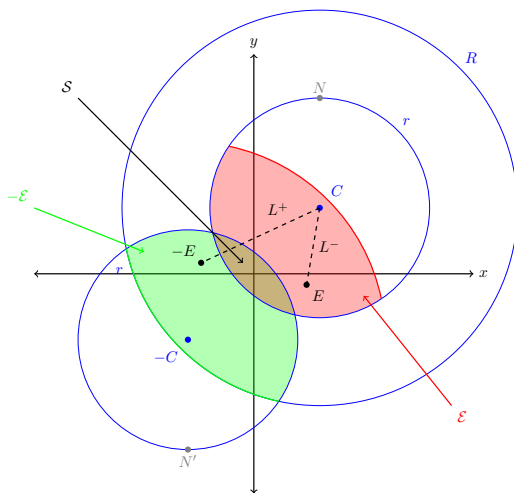


Figure 3: The regions of validity, separability and entanglement for a (maximally-mixed) Group 2 X -state, in the same coordinate system as employed in Figure 2. The points of the closed disc $(-C, r)$ are those of (C, r) when reflected through the origin, as illustrated by the labels N, N' . The regions of entanglement \mathcal{E} and separability $\mathcal{S} = (C, r) \cap (-C, r)$ are shown, with the region of validity $\mathcal{V} = (C, r) \cap (-C, R) = \mathcal{E} \oplus \mathcal{S}$. The state shown is entangled for $(-1)^t \text{sgn}(\beta_0) E \in \mathcal{E}$.

3 X -states as geometric hyperplanes of $\mathcal{W}(3, 2)$

Let us now focus on the symplectic polar space of order two and rank two, $\mathcal{W}(3, 2)$, i.e. the space of all totally isotropic subspaces of $\text{PG}(3, 2)$ with respect to a given symplectic form. The space $\mathcal{W}(3, 2)$ encodes geometrically the commutation relations between the elements of \mathcal{P}_2 in the following sense (see [14]). Given the symplectic form σ of Eq.(4), a totally isotropic line (p, q, r) of $\text{PG}(3, 2)$ is a line such that $\sigma(p, q) = \sigma(p, r) = \sigma(q, r) = 0$. Then any representatives $\mathcal{O}_p, \mathcal{O}_q$ and \mathcal{O}_r of the classes mapped to p, q and r such that (p, q, r) is a totally isotropic line, represent a triple of mutually commuting observables.

$\mathcal{W}(3, 2)$ can also be viewed as a point-line incidence structure $\mathcal{G} = (\mathcal{P}, \mathcal{L}, \mathcal{I})$, where \mathcal{P} are the 15 points and \mathcal{L} are the 15 totally isotropic lines of $\text{PG}(3, 2)$, $\mathcal{I} \subset \mathcal{P} \times \mathcal{L}$ being the incidence relation, i.e. a set-theoretic inclusion of points in lines. The point-line geometry corresponding to $\mathcal{W}(3, 2)$ is a unique triangle-free 15₃-configuration (15 points/lines, 3 points per line and 3 lines through a point) known as the Doily, or the Cremona-Richmond configuration. Restricting to canonical representatives of the classes of \mathcal{P}_2 (i.e. $s = 1$ in Eq. (3)), one obtains one of the ‘standard’ parametrizations of the Doily as illustrated in Figure 4.

Labeled Fano planes were defined as sets of observables commuting with a given observable. The Fano plane of Figure 1 represents the set of observables commuting with ZZ ; geometrically, it is the set of points q of $\text{PG}(3, 2)$ such that $\sigma(p, q) = 0$ for $p = [1 : 0 : 1 : 0]$. In our labeled Doily the trace of the labeled Fano plane corresponds to three concurrent lines; the corresponding set of points is called a perp-set of the point of concurrence. The perp-set of the point ZZ is illustrated in Figure 5. A fact of crucial importance for us is that perp-sets of $\mathcal{W}(3, 2)$ are also geometric hyperplanes of the configuration (Definition 3.1).

Definition 3.1. Let $\mathcal{G} = (\mathcal{P}, \mathcal{L}, \mathcal{I})$ be a point-line incidence structure. A geometric hyperplane H of \mathcal{G} is a subset of \mathcal{P} such that a line of \mathcal{L} is either contained in H , or has just a single point in common with H .

Consider now the hyperbolic quadric of $\mathcal{W}(3, 2)$ defined as:

$$\mathcal{Q}_0 = \{p = [x_1 : x_2 : x_3 : x_4] \in \mathcal{W}(3, 2), x_1x_2 + x_3x_4 + x_1 + x_2 + x_3 + x_4 = 0\}. \quad (13)$$

It is the unique quadric of $\mathcal{W}(3, 2)$ involving only non-trivial Pauli matrices. This quadric is illustrated in red in Figure 6. All quadrics of $\mathcal{W}(3, 2)$ are also geometric hyperplanes in the sense of Definition 3.1.

Definition 3.1 implies that if H_1 and H_2 are two distinct geometric hyperplanes, their intersection $H_1 \cap H_2$ is a geometric hyperplane of the subgeometries defined by H_1 and H_2 . The quadric \mathcal{Q}_0 whose point-line

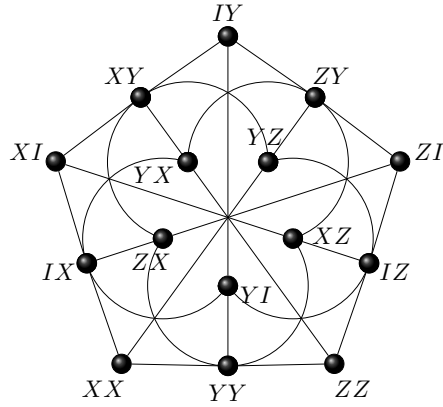


Figure 4: The Doily with its points labeled by two-qubit observables. Two observables commute if they are collinear. Note that lines are represented not only by straight segments, but also by arcs of circles.

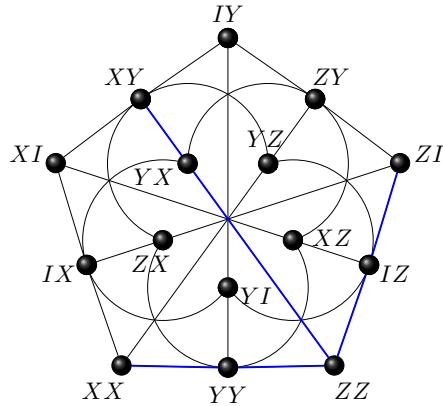


Figure 5: The perp-set (blue) defined by ZZ , which corresponds to the trace on $\mathcal{W}(3, 2)$ of the Fano plane $F_{[1:0:1:0]}$ of $\text{PG}(3, 2)$.

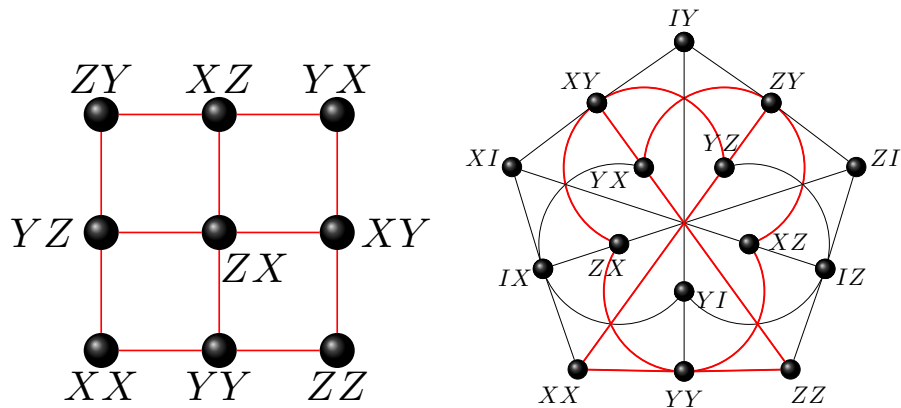


Figure 6: A distinguished hyperbolic quadric in $\mathcal{W}(3, 2)$. Left: Each hyperbolic quadric in $\mathcal{W}(3, 2)$ has the point-line structure of a grid; the quadric in question involves only non-trivial Pauli matrices. Right: The same quadric (red) viewed as a geometric hyperplane of $\mathcal{W}(3, 2)$.

structure can be pictured as a grid (Figure 6) has only two types of geometric hyperplanes, perp-sets and ovoids. Thus the intersections of the 15 perp-sets of $\mathcal{W}(3,2)$ with \mathcal{Q}_0 will be of two different kinds: transverse intersections, corresponding to ovoids (Figure 7) or tangential intersections, corresponding to perp-sets (Figure 8).

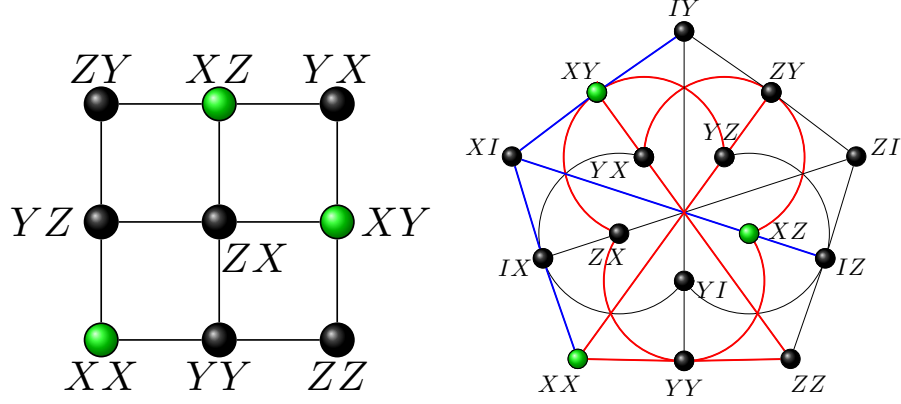


Figure 7: The perp-set H_{XI} of $\mathcal{W}(3,2)$ intersect \mathcal{Q}_0 transversally. Left: $\mathcal{Q}_0 \cap H_{XI}$ (green) is a geometric hyperplane called an ovoid (three points, no two on a line). Right: The same intersection portrayed in $\mathcal{W}(3,2)$.

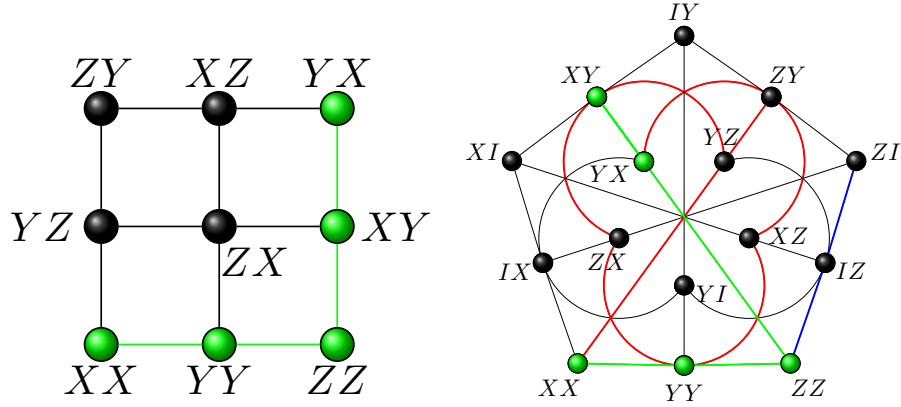


Figure 8: A tangential intersection of \mathcal{Q}_0 with a perp-set (H_{ZZ}) of $\mathcal{W}(3,2)$.

We thus come to a very important observation that furnishes a geometric interpretation of the $9 + 6$ splitting of the X -states described in Section 2.

Proposition 3.2. *The 9 types of X -states of Group 2 correspond to the 9 perp-sets of $\mathcal{W}(3,2)$ that intersect \mathcal{Q}_0 tangentially, whereas the 6 X -states of Group 1 correspond to the 6 perp-sets of $\mathcal{W}(3,2)$ that intersect \mathcal{Q}_0 transversally.*

Proof. The result follows by considering the 15 types of X -states given in Appendix A. \square

4 Hyperplane-states in the two-qubit Pauli group and states with maximally-mixed subsystems

In the previous section we have shown how the 15 distinct sets of two-qubit Pauli observables that generate two-qubit X -states correspond to perp-sets, a specific class of geometric hyperplanes, in $\mathcal{W}(3,2)$ whose points

are parametrized by observables as shown in Figure 4. This leads naturally to considering other geometric hyperplanes of $\mathcal{W}(3,2)$ and the sets of observables lying on them for generating density matrices. Let us make this idea more precise with the following definition:

Definition 4.1. Let ρ be a two-qubit density matrix. One says that ρ is a two-qubit hyperplane-state iff the set of two-qubit observables defining ρ is a geometric hyperplane of $\mathcal{W}(3,2)$.

Example 4.2. X -states are thus a special type of hyperplane-states as they correspond to perp-sets. Let us now consider a density matrix of the form given by Eq. (14).

$$\rho = \frac{1}{4}(I_4 + \beta_{xx}XX + \beta_{xy}XY + \beta_{xz}XZ + \beta_{yx}YX + \beta_{yy}YY + \beta_{yz}YZ + \beta_{zx}XZ + \beta_{zy}YZ + \beta_{zz}ZZ). \quad (14)$$

It corresponds to the generic form of a maximally-mixed two-qubit state. In terms of hyperplane-state description, this density matrix is generated by the quadric \mathcal{Q}_0 .

At this point we need to introduce some more details about geometric hyperplanes of $\mathcal{W}(3,2)$ [15]. There are altogether three kinds of them, namely:

- 15 perp-sets H_p , defined for each point $p \in \mathcal{W}(3,2)$ as $H_p = \{q \in \mathcal{W}(3,2), \sigma(p, q) = 0\}$. We have met several examples of them; they correspond to the 15 types of X -states.
- 10 grids, or Mermin-hyperplanes. Each of them comprise 9 points and 6 lines, with three points per line and two lines through a point. The quadric \mathcal{Q}_0 given by Eq. (13) and portrayed in Figure 6 serves as an illustrative example. If we take this grid embedded in $\mathcal{W}(3,2)$ and rotate it by $2\pi/5$ degrees around the center of the figure, one obtains 4 more grids ($\mathcal{Q}_1, \dots, \mathcal{Q}_4$). Figure 9 shows the second form of a grid embedded in $\mathcal{W}(3,2)$, referred to as \mathcal{Q}_5 . Performing the same rotation as in the previous case yields the four remaining grids $\mathcal{Q}_6, \dots, \mathcal{Q}_9$. One may call such hyperplanes Mermin-hyperplanes, as each of them furnishes an observable-based proof (a Mermin-Peres ‘magic’ square) of the famous Kochen-Specker theorem (see [6] and [9] for the original argument and [15, 10, 2] for the discussions of the geometrical contexts).
- 6 ovoids. An ovoid of $\mathcal{W}(3,2)$ is a set of five points, no two of them being collinear. Figure 9 depicts two ovoids in $\mathcal{W}(3,2)$. The first one, \mathcal{O}_1 , is rotationally invariant. Rotating the second one, \mathcal{O}_2 , by $2\pi/5$ degrees one obtains the remaining 4 ovoids $\mathcal{O}_i, i = 3, \dots, 6$. Like Mermin-hyperplanes, ovoids also underlie a certain family of quantum contextual configurations (namely three-qubit Mermin pentagrams) using the Klein correspondence [13].

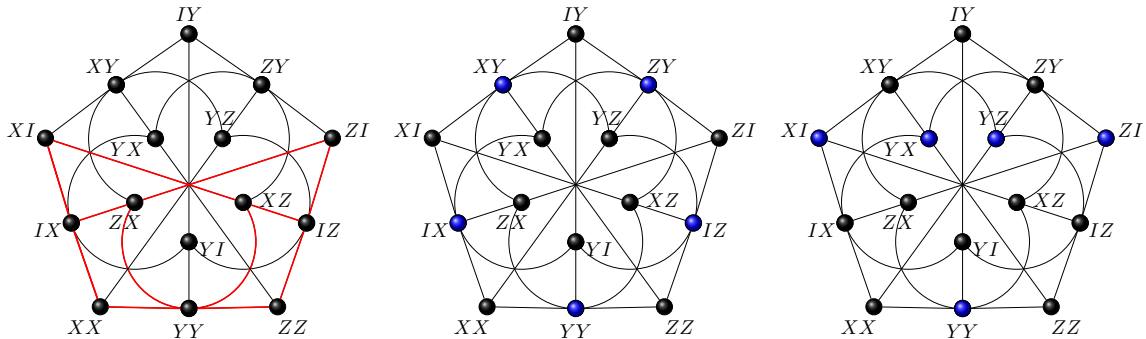


Figure 9: Left: The Mermin-hyperplane denoted as \mathcal{Q}_5 . Its rotation by $2\pi/5$ degrees around the center of the Doily yields four more grids. Middle and Right: The ovoids of $\mathcal{W}(3,2)$. Rotation of the second one by $2\pi/5$ degrees gives four more ovoids.

To each of the 31 geometric hyperplanes listed above one can associate a specific type of two-qubit density matrix. For instance, if one consider the hyperplanes \mathcal{Q}_5 and \mathcal{O}_1 , one gets the following types of quantum

states

$$\rho_{\mathcal{Q}_5} = \frac{1}{4}(I_4 + \tau_x^A XI + \tau_z^A ZI + \tau_x^B IX + \tau_z^B IZ + \beta_{xx}XX + \beta_{YY}YY + \beta_{zz}ZZ + \beta_{zx}ZX + \beta_{xz}XZ) \quad (15)$$

and

$$\rho_{\mathcal{O}_1} = \frac{1}{4}(I_4 + \tau_x^B IX + \tau_z^B IZ + \beta_{xy}XY + \beta_{zy}ZY + \beta_{yy}YY), \quad (16)$$

respectively.

The 10 Mermin-hyperplane states depend generally on 9 parameters, whereas the 6 ovoid-states on 5 parameters. However, if we restrict to states with maximally-mixed subsystems, i.e. states such that their partially reduced states are maximally mixed, $\rho_A = \frac{1}{2}I_2$ and $\rho_B = \frac{1}{2}I_2$, or, in our context, two-qubit density matrices such that the τ coefficients are zero, we arrive at the following result:

Proposition 4.3. *Let us consider the 16-member family of hyperplane-states that is the union of 10 Mermin-hyperplane-states and 6 ovoid-states. Then*

- The \mathcal{Q}_0 -hyperplane states correspond to general two-qubit states with maximally-mixed subsystems.
- The 9 \mathcal{Q}_i -hyperplane states correspond to X -states of Group 2 with maximally-mixed subsystems.
- The 6 \mathcal{O}_i -hyperplane states correspond to X -states of Group 1 with maximally-mixed subsystems.

Proof. A case by case argument leads to the result. \square

5 Non-locality of hyperplane-states

To address non-local properties of hyperplane-states, we will borrow the following theorem from Horodecki et. al. [4]:

Theorem 5.1 (Horodecki R., Horodecki P., Horodecki M. [4]). *A density matrix ρ describes a state that violates the Bell inequality iff $\mathcal{M} > 1$, where $\mathcal{M} = u + \bar{u}$, the sum of the two largest eigenvalues of the matrix $\beta^T \beta$.*

For both Group 1 X -states and ovoid-states, their consistent separability renders them locally realistic for all valid choices of parameters. Concerning Group 2 and Mermin-states $\mathcal{Q}_1, \dots, \mathcal{Q}_9$, we will examine those that share the same β matrices. (As already mentioned, the remaining Mermin-state, \mathcal{Q}_0 , corresponds to the most general 2-qubit states with maximally-mixed subsystems). The eigenvalues u_i of $\beta^T \beta$ can be expressed in terms of generalised parameters (7) as follows

$$u_i = \{\beta_0^2, \frac{1}{2}(B(M) \pm U(M))\}, \quad (17)$$

where $B(M) := \text{Tr} M^T M$ and $U := \sqrt{B^2 - 4(\det M)^2}$. The two eigenvalues $\frac{1}{2}(B \pm U)$ are the eigenvalues of the matrix $M^T M$, which we denote by m_1, m_2 with $m_1 = \frac{1}{2}(B - U)$, and $m_2 = \frac{1}{2}(B + U)$.

One has then in terms of B and U that

$$\mathcal{M} = \begin{cases} B, & \beta_0^2 < m_1, \\ \beta_0^2 + \frac{1}{2}(B + U), & \beta_0^2 \geq m_1. \end{cases} \quad (18)$$

This leads to the following proposition:

Proposition 5.2. *The set of (not necessarily valid) Group 2 X -states or Mermin-states $\{\rho\}$ with given $\beta_0, \beta_3, \beta_4$ and constant \mathcal{M} is given by a connected subset of points on the union of a circle and ellipse centered at the origin, consisting of arcs of the circle within the ellipse, and arcs of the ellipse within the circle (see Fig. 10).*

Proof. Without loss of generality, one can choose generalised coordinates rotated such that $\beta_3 = 0$ and the points $C, -C$ lie on the x -axis.

As m_1, m_2 are eigenvalues of the matrix $M^T M$, one can write the characteristic polynomial of this matrix in generalised coordinates:

$$\begin{aligned} f(\lambda) &= \lambda^2 - \lambda \text{Tr} M^T M + \det M^T M \\ &= \lambda^2 - \lambda(\beta_1^2 + \beta_2^2 + \beta_4^2) + \beta_1^2 \beta_4^2. \end{aligned}$$

Taking an eigenvalue $m \in \{m_1, m_2\}$ as input, this results in

$$\begin{aligned} 0 &= m^2 - m(\beta_1^2 + \beta_2^2 + \beta_4^2) + \beta_1^2 \beta_4^2, \\ &\Rightarrow \frac{\beta_1^2}{m} + \frac{\beta_2^2}{m - \beta_4^2} = 1. \end{aligned} \tag{19}$$

For the denominators in (19) constant one obtains the equations for two conic sections, one for each m_i , $i = 1, 2$. For the denominators both positive, one has the equation for an ellipse, and for the first denominator positive and the second negative, one has the equation for a hyperbola. As m_i are eigenvalues of the square matrix $M^T M$, they are necessarily non-negative, so it suffices to check the sign of $m_i - \beta_4^2$ for $m_i \neq 0$.

First, one must check under what conditions one can retrieve constant denominator terms. For $\mathcal{M} = k$ constant, one has that $\max\{m_1 + m_2, \beta_0^2 + m_2\}$ is constant. Taking each argument individually, $m_1 + m_2 = B = k$ gives (recalling $B = \sum_{i=1}^4 \beta_i^2$):

$$\beta_1^2 + \beta_2^2 = k - (\beta_3^2 + \beta_4^2),$$

i.e. the equation of a circle in coordinates with varying β_1, β_2 and given β_3, β_4 , provided $k > \beta_4^2 + \beta_3^2$. For $k < \beta_3^2 + \beta_4^2$, no such solutions exist, and \mathcal{M} can only be given by $\beta_0^2 + m_2$. One has from proposition 2.2 that a state can be valid only if $\beta_3^2 + \beta_4^2 \leq 1$, so a minimally valid system ($\beta_3^2 + \beta_4^2 = 1$) allows only $B \geq 1$.

Taking the other argument, $\beta_0^2 + m_2$ constant for given β_0 indicates that m_2 is constant, which provides constant denominators in (19). One can recover that $m_2 - \beta_4^2 \geq 0$ by assuming the negation, and substituting the β_i terms into m_2 , with $\beta_3 = 0$. One then obtains $(\beta_2 \beta_4)^2 < 0$, a contradiction. This then provides via (19) the equation for an ellipse, with semi-major and semi-minor axes given by $a = \sqrt{m_2}$ and $b = \sqrt{m_2 - \beta_4^2}$, respectively, and foci at $\pm C = (\pm \beta_4, 0)$.

(Note that the term $m_1 - \beta_4^2$ can be similarly examined and found to be non-positive, however the constancy conditions on \mathcal{M} do not give a constant m_1 term so the hyperbola given by substituting m_1 into (19) does not arise in this examination).

The curves of constant $m_1 + m_2$, $\beta_0^2 + m_2$ are then given by a circle and an ellipse, respectively (see Fig. 10). The curve of constant $\mathcal{M} = \max\{m_1 + m_2, \beta_0^2 + m_2\}$ is given by the sections of these curves that lie within the alternate conic section, i.e. the arcs of the circle that lie within the ellipse, and the arcs of the ellipse that lie within the circle. To see this, consider a point p on the curve $\mathcal{M} = k$. p must then be on either the circle or the ellipse, whichever has maximal value at that point. This requires that the *other* curve has value less than k at the point p . Curves of constant B are given by circles centred at the origin, with increasing radii for increasing constant value. The same is true for curves of constant $\beta_0^2 + m_2$, i.e. ellipses centred at the origin with increasing semi-major and semi-minor axes for increasing constant value. Thus, for one curve to have value k and one curve to have value less than k at the point p , we require that p is contained on one curve and *inside* the other, for any p on the curve $\mathcal{M} = k$. Thus, it is given by arcs of the circle contained within the ellipse, and vice-versa. □

The set of locally realistic states then lie in the closed region bounded by \mathcal{V} and the curve given by $\mathcal{M} = 1$ (see Fig. 11, and note that $\beta_3 \neq 0$ in this graph).

The four intersection points (when they exist) of these curves are found to be at $(\pm \hat{\beta}_1, \pm \hat{\beta}_2)$, where

$$\hat{\beta}_1 = \sqrt{m_1 m_2} / \beta_4,$$

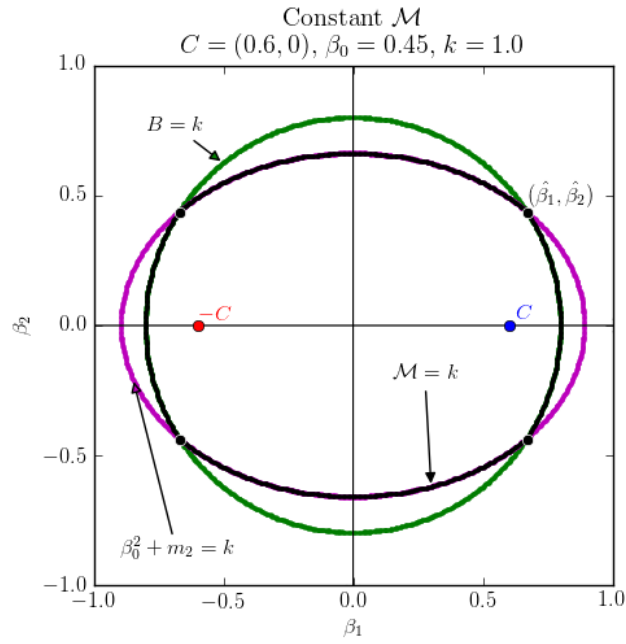


Figure 10: Curves of constant $\mathcal{M} = k$ for $k = 1$, $C = (\beta_4, \beta_3) = (0.6, 0)$, $\beta_0 = 0.45$. The curve of constant $B = 1$ is given by the green circle with radius $r_B = \sqrt{1 - \beta_4^2} = 0.8$. The curve of constant $\beta_0^2 + m_2 = 1$ is given by the pink ellipse with foci at $\pm C$ and semi-major and semi-minor axes given by (respectively) $a = \sqrt{m_2} \approx 0.893$, $b = \sqrt{m_2 - \beta_4^2} \approx 0.661$. The curve of constant $\mathcal{M} = 1$ is given by the union of the arcs of the circle contained within the ellipse, and the arcs of the ellipse contained within the circle (black curve). The intersection points are given by $(\pm\hat{\beta}_1, \pm\hat{\beta}_2)$.

$$\hat{\beta}_2 = \sqrt{-(m_1 - \beta_4^2)(m_2 - \beta_4^2)}/\beta_4.$$

As the circle and ellipse are both centred on the origin, they intersect only when the circle radius $r_B = \sqrt{k - \beta_4^2}$ is valued between the semi-major and semi-minor axes a, b . This can be expressed in terms of k :

$$m_2 \leq k \leq m_2 + \beta_4^2. \quad (21)$$

One can immediately note that $k = m_1 + m_2$ cannot fall below the lower bound above. For k above the upper bound, the circle $B = k$ entirely surrounds the ellipse, and the curve $\mathcal{M} = k$ is given by only the ellipse.

For Group 2 X -states with general τ 's, one can compute an upper bound for \mathcal{M} using the validity criteria, which when written in terms of B and $\det M$ give us (for type I states):

$$\sqrt{B - 2\det M + (\tau_1 + \tau_2)^2} \leq 1 + \beta_0, \quad (22a)$$

$$\sqrt{B + 2\det M + (\tau_1 - \tau_2)^2} \leq 1 - \beta_0. \quad (22b)$$

Combining these to get conditions on B and U and taking sign transformations on τ_2 and β_0 to account for type II states, one obtains

$$\begin{aligned} B &\leq 1 + \beta_0^2 - (\tau_1^2 + \tau_2^2), \\ U^2 &\leq (1 - \beta_0^2)^2 - 2B(\tau_1^2 + \tau_2^2) - (-1)^t 8\tau_1\tau_2\det M, \end{aligned}$$

which give the following upper bound on \mathcal{M} :

$$\mathcal{M} \leq \beta_0^2 + \frac{1}{2} \left(1 + \beta_0^2 - (\tau_1^2 + \tau_2^2) + \sqrt{(1 - \beta_0^2)^2 - 2B(\tau_1^2 + \tau_2^2) - (-1)^t 8\tau_1\tau_2\det M} \right). \quad (23)$$

When $\tau_i = 0$ this reduces to $\mathcal{M}_{\tau=0} \leq 1 + \beta_0^2$, which also holds for the nine Mermin-states \mathcal{Q}_i , as they differ from Group 2 X -states only by their τ -parameters. Saturating this bound to the maximal case $\mathcal{M} = 2$ is a necessary and sufficient condition for purity, as can be shown:

Proposition 5.3. *For ρ being a Group 2 X -state or one of the nine \mathcal{Q}_i -states with $\tau_i = 0$, it violates the Bell Inequality maximally iff is pure.*

Proof. It is known [3] that a state written in Pauli operator form is pure (i.e. $\text{Tr}(\rho^2) = 1$) iff $\sum_i \tau_i^2 + \sum_{i,j} \beta_{ij}^2 = 3$. For our considerations this reduces to $\beta_0^2 + B = 3$ (recall that $B = \sum_{i=1}^4 \beta_i^2$).

(\Rightarrow) Allowing the state to be maximally nonlocal, one has that $\mathcal{M} = 2$ and thus by the upper bound given above, $\beta_0^2 = 1$. For the former case in (18), maximal nonlocality gives $B = 2$ and thus purity. For the latter case, the validity conditions (22) with $|\beta_0| = 1$ give $B = \pm 2\det M$, and then $U = 0$. Then one has

$$\begin{aligned} \mathcal{M} &= \beta_0^2 + \frac{1}{2}(B + U), \\ \Rightarrow 2 &= 1 + B/2 \Rightarrow B = 2, \end{aligned}$$

giving $\beta_0^2 + B = 3$.

(\Leftarrow) Taking the former case in (18), one can write $\mathcal{M} = B = 3 - \beta_0^2$. It is known that \mathcal{M} is at most 2 [4] and it can be seen by the validity conditions that $|\beta_0|$ is at most 1. $\mathcal{M} = 3 - \beta_0^2$ then requires that $\beta_0^2 = 1$, and $\mathcal{M} = 2$. For the latter case in (18), one squares and adds the validity conditions (22) to get

$$\begin{aligned} 1 + \beta_0^2 &\geq B = 3 - \beta_0^2, \\ \Rightarrow \beta_0^2 &\geq 1, \end{aligned}$$

as $|\beta_0|$ is at most 1, one recovers that $\beta_0^2 = 1$ and thus $B = 2$. By the previous argument, $\beta_0^2 = 1 \Rightarrow U = 0$ and then $\mathcal{M} = 1 + 2/2 = 2$. \square

One thus recovers the fact that the known examples of two-qubit states that maximally violate Bell-inequality are pure [4] and, as also indicated by several other studies, that for mixed states a large amount of entanglement seems to be necessary to obtain violation of Bell-inequalities [7]. Using our description of X -states of Group 2 and Mermin states with generalised parameters, one can represent the region of entanglement and violation of Bell-inequality in the parameter space of Figures 2 and 3 as depicted in Figure 11:

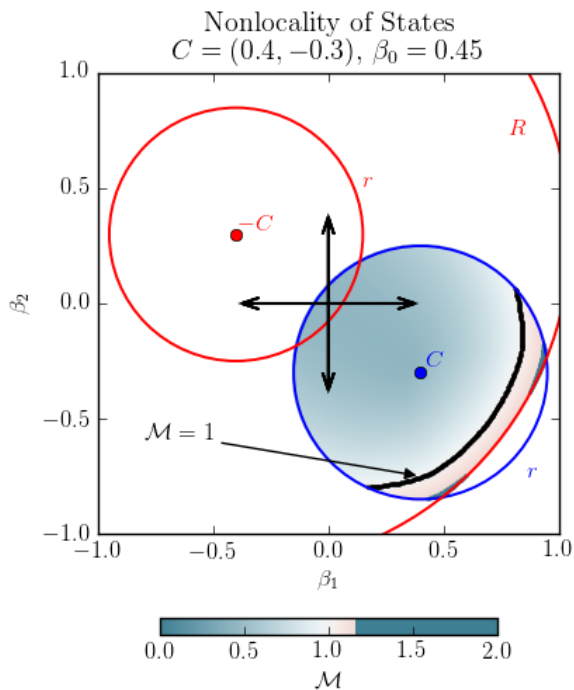


Figure 11: Graph of nonlocality measure \mathcal{M} for various hyperplane states with $\tau_i = 0$, $C := (\beta_4, \beta_3) = (0.4, -0.3)$ and $\beta_0 = 0.45$. Values of β_1 and β_2 are plotted on the x, y -axes, respectively. Values for \mathcal{M} are computed for states within the validity region $\mathcal{V} = (C, r) \cap (-C, R)$ and given by the red-blue scale. A set of states parametrised by constant \mathcal{M} forms an ellipse with focal points at $C, -C$ in the plane, the example $\mathcal{M} = 1$ shown in black (for the subset within \mathcal{V}). As can be seen, only a small proportion of valid states are nonlocal ($\mathcal{M} > 1$), and a high amount of entanglement is needed to satisfy this condition.

6 Conclusion

In this paper we have considered the 15 types of X -states following a remark of Rau [11] who suggested to define X -states from the algebraic structure of the defining two-qubit operators used to decompose the state in the Pauli basis. We showed that these 15 types split in two groups 9+6 when we consider their entanglement properties. The Group 2 (9 types) is the only one that can produce entangled states. A uniform treatment of those states is proposed and some criteria in terms of their parameters have been proposed for states with maximally-mixed subsystems. The introduction of those parameters allows us to give a representation of the validity, entanglement and Bell-violation area. One also proposed an alternative geometric definition of X -states as perp-hyperplanes of the symplectic polar space $\mathcal{W}(3, 2)$. This new definition establishes an interesting connection between the finite geometric picture introduced in quantum information to study configuration of two-qubit operator and the two-qubit density matrices. In particular, we started to study hyperplanes-states, i.e. density matrices which involve two-qubit operators defining a geometric hyperplane. In this line many questions related to the concepts of Veldkamp line and Veldkamp space, the space of geometric hyperplanes [15], can be addressed. When we restrict ourself to density matrices with maximally-mixed subsystems one observed that all hyperplane-states of $\mathcal{W}(3, 2)$ coincide with the generalised X -states with maximally mixed subsystems. However, if one does not consider the restriction on the subsystems, Mermin-states and X -states are not equivalent anymore and it could be interesting in a future work to differentiate those states in terms of their quantum properties. Another direction would be to consider three-qubit X -states where similar algebraic structure show up [17] and where the finite geometric picture of the three-qubit Pauli group reveals fascinating properties [5, 16].

Acknowledgments

This work was supported, in part, by the Slovak Research and Development Agency under the contract # SK-FR-2017-0002, as well as by the Slovak VEGA Grant Agency, Project # 2/0004/20. This work was also supported by the National Research Development and Innovation Office of Hungary within the Quantum Technology National Excellence Program (Project No. 2017-1.2.1-NKP-2017-0001). In France the project was supported by the French ‘‘Investissements d’Avenir’’ programme, project ISITE-BFC (contract ANR-15-IDEX-03) and the EUR-EIPHI Graduate School (Grant No. 17-EURE-0002).

A The 15 Fano planes of $\text{PG}(3, 2)$

The geometry of $\text{PG}(3, 2)$ comprises 15 points, 35 lines and 15 planes. All the 15 planes corresponding to 15 types of X -states can be labelled by the 15 points as explained in the introduction:

$$F_p = \{q \in \text{PG}(3, 2), \sigma(p, q) = 0\}. \quad (24)$$

For the convenience of the reader we provide in Table 1 the explicit list of the 15 Fano planes of $\text{PG}(3, 2)$ with respect to the Group 1/2 splitting.

| Group | $p \in \text{PG}(3, 2)$ | F_p |
|-------|--------------------------------------|------------------------------|
| 1 | $[0 : 0 : 0 : 1] \leftrightarrow IX$ | $XX, YX, ZX, XI, YI, ZI, IX$ |
| | $[0 : 0 : 1 : 0] \leftrightarrow IZ$ | $XZ, YZ, ZZ, XI, YI, ZI, IZ$ |
| | $[0 : 0 : 1 : 1] \leftrightarrow IY$ | $XY, YY, ZY, XI, YI, ZI, IY$ |
| | $[0 : 1 : 0 : 0] \leftrightarrow XI$ | $XX, XY, XZ, IX, IY, IZ, XI$ |
| | $[1 : 0 : 0 : 0] \leftrightarrow ZI$ | $ZX, ZY, ZZ, IX, IY, IZ, ZI$ |
| | $[1 : 1 : 0 : 0] \leftrightarrow YI$ | $YX, YY, YZ, IX, IY, IZ, YI$ |
| 2 | $[0 : 1 : 0 : 1] \leftrightarrow XX$ | $XX, YY, YZ, ZY, ZZ, IX, XI$ |
| | $[0 : 1 : 1 : 0] \leftrightarrow XZ$ | $XZ, YY, YX, ZX, ZY, IZ, XI$ |
| | $[0 : 1 : 1 : 1] \leftrightarrow XY$ | $XY, YX, YZ, ZX, ZZ, IY, XI$ |
| | $[1 : 0 : 0 : 1] \leftrightarrow ZX$ | $ZX, XY, XZ, YY, YZ, IX, ZI$ |
| | $[1 : 0 : 1 : 0] \leftrightarrow ZZ$ | $ZZ, YY, XX, XY, YX, IZ, ZI$ |
| | $[1 : 0 : 1 : 1] \leftrightarrow ZY$ | $ZY, XX, XZ, YX, YZ, IY, ZI$ |
| | $[1 : 1 : 0 : 1] \leftrightarrow YX$ | $YX, XY, XZ, ZY, ZZ, IX, YI$ |
| | $[1 : 1 : 1 : 0] \leftrightarrow YZ$ | $YZ, XX, XY, ZX, ZY, IZ, YI$ |
| | $[1 : 1 : 1 : 1] \leftrightarrow YY$ | $YY, XX, XZ, ZX, ZZ, IY, YI$ |

Table 1: The 15 Fano planes of $\text{PG}(3, 2)$ according to the Group 1/2 splitting.

References

- [1] Qing Chen, Chengjie Zhang, Sixia Yu, XX Yi, and CH Oh. Quantum discord of two-qubit X states. *Physical Review A*, 84(4):042313, 2011.
- [2] Frédéric Holweck and Metod Saniga. Contextuality with a small number of observables. *International Journal of Quantum Information*, 15(04):1750026, 2017.
- [3] Michał Horodecki, Paweł Horodecki, and Ryszard Horodecki. Separability of n-particle mixed states: necessary and sufficient conditions in terms of linear maps. *Physics Letters A*, 283(1-2):1–7, 2001.
- [4] Ryszard Horodecki, Paweł Horodecki, and Michał Horodecki. Violating Bell inequality by mixed spin-1/2 states: necessary and sufficient condition. *Physics Letters A*, 200(5):340–344, 1995.
- [5] Péter Lévy, Frédéric Holweck, and Metod Saniga. Magic three-qubit Veldkamp line: A finite geometric underpinning for form theories of gravity and black hole entropy. *Physical Review D*, 96(2):026018, 2017.

- [6] N David Mermin. Hidden variables and the two theorems of John Bell. *Reviews of Modern Physics*, 65(3):803, 1993.
- [7] WJ Munro, K Nemoto, and AG White. The Bell inequality: A measure of entanglement? *Journal of modern optics*, 48(7):1239–1246, 2001.
- [8] Michael A Nielsen and Isaac Chuang. *Quantum computation and quantum information*. Cambridge University Press, 2002.
- [9] Asher Peres. Two simple proofs of the Kochen-Specker theorem. *Journal of Physics A: Mathematical and General*, 24(4):L175, 1991.
- [10] Michel Planat and Metod Saniga. On the Pauli graphs of N-qudits. *Quant. Inf. Comput.*, 8(quant-ph/0701211):127–146, 2007.
- [11] ARP Rau. Algebraic characterization of X-states in quantum information. *Journal of Physics A: Mathematical and Theoretical*, 42(41):412002, 2009.
- [12] ARP Rau. Mapping two-qubit operators onto projective geometries. *Physical Review A*, 79(4):042323, 2009.
- [13] Metod Saniga and Péter Lévay. Mermin’s pentagram as an ovoid of PG(3,2). *EPL (Europhysics Letters)*, 97(5):50006, 2012.
- [14] Metod Saniga and Michel Planat. Multiple Qubits as Symplectic Polar Spaces of Order Two. *Advanced Studies in Theoretical Physics*, 1:1–4, 2007.
- [15] Metod Saniga, Michel Planat, Petr Pracna, Hans Havlicek, et al. The Veldkamp space of two-qubits. *SIGMA. Symmetry, Integrability and Geometry: Methods and Applications*, 3:075, 2007.
- [16] Metod Saniga and Zsolt Szabó. Magic Three-Qubit Veldkamp Line and Veldkamp Space of the Doily. *Symmetry*, 12(6):963, 2020.
- [17] Sai Vinjanampathy and ARP Rau. Generalized X states of N qubits and their symmetries. *Physical Review A*, 82(3):032336, 2010.
- [18] Ting Yu and JH Eberly. Evolution from entanglement to decoherence of bipartite mixed "X" states. *arXiv preprint quant-ph/0503089*, 2005.